Proceedings of the ASME 2013 Conference on Smart Materials, Adaptive Structures and Intelligent Systems
SMASIS2013
September 16-18, 2013, Snowbird, Utah, USA

SMASIS2013-3267

ON THE CONTROL OF A DIELECTRIC ELASTOMER ARTIFICIAL MUSCLE WITH VARIABLE IMPEDANCE

Gianluca Palli[1], **Giovanni Berselli**[2*]
[1]University of Bologna, Viale Risorgimento 2, 40136 Bologna, Italy, e-mail: gianluca.palli@unibo.it
[2]University of Modena and Reggio Emilia, Via Vignolese 905, 41125 Modena, Italy, e-mail: giovanni.berselli@unimore.it

ABSTRACT

Artificial Muscles based on Dielectric Elastomers (DE) can potentially enable the realization of bio-inspired actuation systems whose intrinsic compliance and damping can be varied according to the task requirements. Nonetheless, the control of DE-based Variable Impedance Actuators (VIA) is not trivial owing to the non-linear viscoelastic response which characterizes the acrylic dielectrics commonly employed in practical devices.
In this context, the purpose of the present paper is to outline a novel strategy for the control of DE-based VIA. Although the proposed methodology is applicable to generic DE morphologies, the considered system is composed of a couple of conically-shaped DE films in agonistic-antagonistic configuration. Following previously published results, the system dynamic model is firstly recalled. Then, a DE viscoelasticity compensation technique is outlined together with a control law able to shape the DE actuator impedance as desired. The operative limits of the system are explicitly considered and managed in the controller by increasing the operating DE actuator stiffness if required. In addition, the problem of model uncertainties compensation is also addressed. Finally, as a preliminary step towards the realization of a practical DE-based VIA, the proposed control approach is validated by means of simulations.

*Corresponding author
This research has been partially funded by InterMech MO.RE. Laboratory, Advanced Mechanics and Engine Design Research Center, Regione Emilia Romagna and by the Interdepartmental Center for Industrial Research on Advanced Applications in Mechanical Engineering and Materials (CIRI-MAM), within the framework of the Programma Operativo POR-FESR 2007-2013 of Regione Emilia-Romagna, Italy.

1 INTRODUCTION

In the last decade, a great deal of economic and scientific effort has been devoted to the introduction of service robots in the fields of medicine, security, defense, entertainment, and also in more traditional working environments [1]. Differently from industrial robots for the manufacturing industry, which are designed so as to achieve fast and accurate positioning of the manipulated parts, service robots are characterized by less demanding accuracy requirements but should ensure a suitable level of safety and dependability during the interaction/collaboration with humans.
In particular, recent research activities (e.g. [2, 3]) showed that standard actuation and control technologies, along with traditional design paradigms originally developed for industrial machines and mainly devoted to structural stiffness maximization, are not suited for dealing with tasks involving unstructured human-robot or robot-environment interaction (such as the manipulation of unknown/fragile objects or the locomotion in rough terrains). The major limits shown by traditional actuators (e.g. electric rotary motors and gearboxes) are the small power-to-weight ratio, the large inertia and mechanical impedance, the poor (force and position) accuracy at low speeds, and the limited resilience and damage resistance [4].
On the other hand, interactive tasks are well performed by animals, which are able to modulate their joint impedance by the simultaneous activation of two actuators placed in agonistic-antagonistic configuration (the differential activation of the same muscles resulting in a joint position change [5]). For instance, as previously highlighted by several authors (e.g. [6, 7], the modulation of the actuator stiffness can be used for achieving a stable

interaction with unknown environments also in presence of disturbances or impulsive forces (e.g. catching an object or landing from a jump [8, 9]) or for increasing energy efficiency during locomotion [10]. In addition, stiffness tuning can be employed to obtain a suitable trade-off between accuracy and safety when robot tasks are performed in the proximity of humans. In particular, compliant actuators with tunable properties might be used to lower possible injuries in case of accidental impacts, by ensuring high structural stiffness for robot operating a slow velocities and high compliance in case of fast motion [11]. For instance, the simultaneous decoupled control of position and stiffness in a manipulators equipped with variable stiffness actuators is discussed in [12], whereas a torque and stiffness controller in an antagonistic pneumatic system can be found in [13].

For what concerns the practical implementation of variable stiffness and Variable Impedance Actuators (VIA), an impressively high number of design solutions have been proposed in the last few years. These different prototypes may be mainly classified into the aforementioned antagonistic systems (e.g. [14–16]) where a couple of actuators is used to simultaneously adjust position and stiffness, and structure-controlled systems (e.g. [17,18]), where the stiffness modulation relies on the change in geometry of some passive spring. Variable impedance has also been obtained by means of elctro/magneto-rheological devices (e.g. [19] and pneumatic systems (e.g. [13]).

In this context, Dielectric Elastomers (DE) Artificial Muscles can potentially enable the realization of bio-inspired VIA thanks to their intrinsic compliance and damping, large power densities, low costs, and shock-insensitivity. As known, DE are deformable dielectrics, which can experience finite deformations in response to large electric fields. In electromechanical transducers (actuators, sensors [20] and generators [21]), DE are generally shaped in thin sheets coated with compliant electrodes on both sides. From an electrical standpoint, DE are deformable capacitors in which the electrical parameters (resistance/capacity) vary as a function of the imposed deformation.

In particular, the purpose of the present paper is to outline a novel strategy for the control of DE-based VIA. The considered VIA prototype, previously presented by the authors in [22], is composed of a couple of conically-shaped DE films in agonistic-antagonistic configuration (see Fig. 1 and 2). At first, the nonlinear visco-elastic model of the system is briefly recalled for clarity. Then, a DE viscoelasticity compensation technique is outlined together with a control law able to shape the DE actuator impedance as desired. The control system, which relies on the actuator position information and on the measurement of the interaction force, is composed of: 1) an observer of the DE films internal state that allows compensating for the viscoelastic effects; 2) a controller that shapes the actuator impedance and modulates the stiffness for ensuring system controllability; 3) an observer for the estimation and the compensation of model uncertainties.

2 VARIABLE IMPEDANCE ACTUATOR DESIGN

Recalling the VIA design published in [22], the actuator CAD model and physical prototype are depicted in Fig. 1 and 2, respectively. The considered system comprises:

- A rigid frame made of two coaxial identical rings with internal radii equalling $r_M = 40mm$ and connected by four rods with lengths equalling $2d = 40mm$;
- Two conically-shaped DE films (film #1 and film #2) connecting the two rigid frame rings to a rigid platform (i.e. the actuator output) in an agonist-antagonist arrangement (the platform having an external radius equalling $r_m = 12mm$).

Each DE film is a circular membrane of acrylic elastomer (VHB-4905 by 3M) with initial thickness (in its undeformed state) equalling $t_0 = 1.5mm$, subjected to an equibiaxial pre-stretch equalling $\lambda_p = 4$, and coated with a pair of compliant carbon conductive grease electrodes. These virgin membranes are then subjected to preconditioning loading-unloading cycles resulting in a residual stretch (permanent set, $\lambda_r = 1.6$) whose value has been estimated on sacrificial specimen. A voltage difference V_1 (V_2) between the electrode pair of the DE film #1 (#2) generates a downward (upward) force on the actuator output.

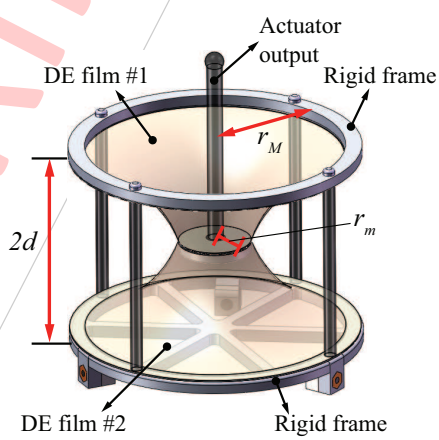

Figure 1. DE-based VIA CAD model.

Figure 2. DE-based VIA physical prototype.

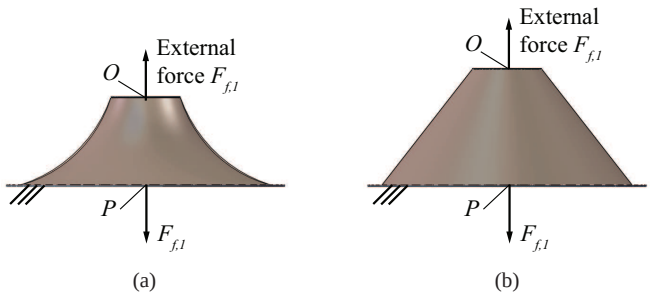

Figure 3. Single actuator CAD model in deactivated (c) and activated (d) states.

3 SYSTEM DYNAMICS

3.1 Background on conical DE actuators models

Figure 3 depicts a schematic of a single actuator in its deactivated and activated states respectively. It can be noticed that the DE-film is characterized by a concave conical shape (Fig. 3(a)) whose curvature decreases upon activation (Fig. 3(b)). In particular, differently from other modeling methods [23, 24], the procedure described in [25] i relies on the assumption that the incompressible DE is a right circular cone with constant wall thickness (like Fig. 3(b)) in any of its deformed configurations. Let then first consider, for instance, the DE film #1. The expression of the overall external force, $F_{f,1}$, that must be supplied at O and P (and directed along the line joining these points, Fig. 3) to balance the DE internal reaction force at a given generic configuration x of the actuator, can be expressed as:

$$F_{f,1}(x,\dot{x},V_1) = F_{ve,1}(x,\dot{x}) - F_{em,1}(x,V_1) \tag{1}$$

where $F_{ve,1}$ represents the viscoelastic response of the DE film and $F_{em,1}$ represents the so-called *Maxwell force* [26, 27].
A suitable expression for the latter term, $F_{em,1}$, is given by [28]:

$$F_{em,1}(V_1,x) = \chi x \pi^2 V_1^2 (r_M + r_m)^2 \varepsilon \Big/ \nu \tag{2}$$

where $\nu = \pi(r_M^2 - r_m^2)t_0\ \lambda_p^{-2}$ is the DE volume, $\varepsilon = 4.5 \cdot 8.85e-12$ is the dielectric permittivity of the acrylic film, and $\chi = 0.6$ is a suitable dimensionless correction factor accounting for the aforementioned geometrical approximation (i.e. the DE always assumed as a right circular cone). As for the DE viscoelastic response, a possible approach is to resort to a one dimensional Quasi-Linear Viscoelastic (QLV) model [29]. Henceforth, it is supposed that the force produced by an infinitesimal displacement $dx(\tau)$, superposed in a state of displacement x at an instant of time τ, is, for $\tau > t$:

$$dF_{ve,1}(t) = g(t-\tau)\frac{dF_{e,1}[x(\tau)]}{dx}dx(\tau) \quad \text{with} \quad g(0) = 1 \tag{3}$$

where, having assumed $x = 0$ for $t < 0$ and a differentiable displacement history, $F_{e,1}(x)$ is the *elastic response*, i.e. the force generated by an instantaneous displacement, whereas $g(t)$ is the *reduced relaxation function*, which describes the time-dependant behavior of the material. A suitable expression for $g(t)$ is given by:

$$g(t) = \sum_{i=0}^{r} c_i e^{-\nu_i \cdot t} \quad \text{with} \quad \sum_{i=0}^{r} c_i = 1 \tag{4}$$

where the coefficients c_i depend on the employed material whereas the coefficients ν_i identify the rate of the relaxation phenomena (in general, $\nu_0 = 0$). Finally, the total force at the instant t is the sum of the contributions due to all the past changes [30], i.e.

$$\begin{aligned} F_{ve,1}(t) &= \int_0^t g(t-\tau)\, K_{e,1}[x(\tau)]\, \dot{x}(\tau) d\tau \\ &= \int_0^t K_{e,1}(x) \cdot \left[c_0 + \sum_{i=1}^{r} c_i e^{-\nu_i (t-\tau)} \right] \cdot \dot{x}(\tau) d\tau \end{aligned} \tag{5}$$

having defined $K_{e,1}(x) = \partial F_{e,1}[x]/\partial x$. In particular, referring to Fig. 4, the force response given by the QLV model can be interpreted as that of a nonlinear stiffness connected by a series of r linear Kelvin models (i.e. a parallel spring-damper system). Concerning the DE quasi-static response, $F_{qs,1}$, a suitable expression is given by [28]:

$$\begin{aligned} F_{qs,1}(x) =& c_0 F_{e,1} = \xi \nu \left[\sum_{i=1}^{3} i C_i (\lambda_1^2 + \lambda_2^2 + \lambda_1^{-2}\lambda_2^{-2} - 3)^{i-1} \right] \cdot \\ & \cdot (\lambda_1\lambda_2 - \lambda_1^{-3}\lambda_2^{-1}) x \Big/ \left[(r_M - r_m)) \sqrt{x^2 + (r_M - r_m)^2} \right] \end{aligned} \tag{6}$$

where $\lambda_2 = \lambda_p/\lambda_r$ and $\lambda_1 = \lambda_2\sqrt{1 + x^2 \big/ (r_M - r_m)^2}$ are the longitudinal and latitudinal stretches of the DE middle surface, $C_1 = 30488Pa$, $C_2 = 151Pa$, $C_3 = 8Pa$ are DE constitutive parameters of a Yeoh-type hyperelastic strain-energy function [31], and $\xi = 0.93$ is a dimensionless correction factor. This latter term, similarly to the coefficient χ in Eq. 2, accounts for the errors introduced by the simplifying assumption of the DE being a right circular cone. Concerning the reduced relaxation function, $r = 3$, $c_0 = 0.83$, $c_1 = 0.22$, $c_2 = 1 - c_1 - c_0$, $\nu_1 = 4.30s^{-1}$, $\nu_2 = 0.70s^{-1}$. Note that the elastic (instantaneous) response, $F_{e,1}$, is simply found by multiplication of the quasi-static response, $F_{qs,1}$, by the constant c_0 (where $c_0 < 1$).

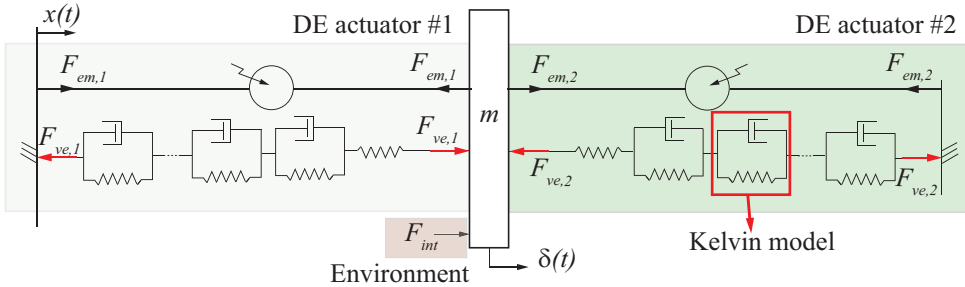

Figure 4. Actuator non-linear lumped parameter model.

3.2 Dynamics of the overall actuator

Concerning the agonistic-antagonistic actuator, denoting δ as the actuator output position measured from the OFF-state rest location along its axial direction $x = d$ (hereafter this location is referred to as actuator central position), the overall actuator force will be given by:

$$m\ddot{\delta} + F_{f,1}(d+\delta, V_1, t) - F_{f,2}(d-\delta, V_2, t) = F_{\text{int}} \tag{7}$$

where, with obvious notation, $F_{f,2} = F_{ve,2} + F_{em,2}$ is the reaction force of the DE film #2, F_{int} is the interaction force, and m represents an inertial load acting on the VIA output (refer to Fig. 4). By explicitly considering the viscoelastic and electric effects of the DE films, one can write:

$$\begin{aligned} &m\ddot{\delta} + F_{\text{ve},1}(t) - F_{\text{ve},2}(t) + \\ &\quad - F_{\text{em},1}(d+\delta, V_1) + F_{\text{em},2}(d-\delta, V_2) = F_{\text{int}} \end{aligned} \tag{8}$$

The electric effects can be expressed as:

$$F_{\text{em},1}(d+\delta, V_1) = \alpha[d+\delta]V_1^2 \tag{9}$$

$$F_{\text{em},2}(d-\delta, V_2) = \alpha[d-\delta]V_2^2 \tag{10}$$

$$\alpha = \chi\pi^2(r_M + r_m)^2\varepsilon \big/ \nu \tag{11}$$

On the basis of Eq. 5 and by summing the effects of the two DE films, the viscoelastic force can be also written as:

$$\begin{aligned} F_{\text{ve}}(t) &= F_{\text{ve},1}(t) - F_{\text{ve},2}(t) \\ &= \int_0^t g(t-\tau)\frac{\partial\{F_{\text{e},1}[d+\delta(\tau)] - F_{\text{e},2}[d-\delta(\tau)]\}}{\partial\tau}d\tau \\ &\int_0^t g(t-\tau)\frac{\partial F_e[\delta(\tau)]}{\partial\tau}d\tau = \int_0^t g(\tau)\frac{\partial F_e[\delta(t-\tau)]}{\partial\tau}d\tau \end{aligned} \tag{12}$$

and integrating by parts:

$$F_{\text{ve}}(t) = g(t)F_{\text{e}}[\delta(0)] - g(0)F_{\text{e}}[\delta(t)] - \int_0^t \frac{\partial g(\tau)}{\partial\tau}F_{\text{e}}[\delta(t-\tau)]d\tau \tag{13}$$

This last equation represents the response of a linear system with input $F_{\text{e}}[\delta(t)]$ and output $F_{\text{ve}}(t)$. Then, by introducing γ as the internal state of the DE film, the overall viscoelastic force of the DE actuator can be expressed by means of the linear system:

$$\dot{\gamma} = A_{\text{ve}}\gamma + B_{\text{ve}}F_{\text{e}}(\delta) \tag{14}$$

$$F_{\text{ve}}(\delta,\gamma) = C_{\text{ve}}\gamma + D_{\text{ve}}F_{\text{e}}(\delta) \tag{15}$$

where

$$F_{\text{e}}(\delta) = F_{\text{e},1}(d+\delta) - F_{\text{e},2}(d-\delta) \tag{16}$$

$$F_{\text{ve}}(\delta,\gamma) = F_{\text{ve},1}(t) - F_{\text{ve},2}(t) \tag{17}$$

$$A_{\text{ve}} = -\text{diag}[v_1 \ \cdots \ v_r], \quad B_{\text{ve}} = -[v_1 c_1/c_0 \ \cdots \ v_r c_r/c_0]^T \tag{18}$$

$$C_{\text{ve}} = [1 \ \cdots \ 1], \quad D_{\text{ve}} = 1 + \sum_{i=1}^{r} c_i/c_0 \tag{19}$$

This model allows resembling both the instantaneous and the quasi-static (elastic) response of the DE actuator.
Also the electric terms can be suitably grouped together:

$$\begin{aligned} F_{\text{em}}(\delta, V_1, V_2) &= -F_{\text{em},1}(d+\delta, V_1) + F_{\text{em},2}(d-\delta, V_2) \\ &= \alpha d[-V_1^2 + V_2^2] - \alpha\delta[V_1^2 + V_2^2] \end{aligned} \tag{20}$$

Then, the overall DE actuator dynamics can be written as:

$$m\ddot{\delta} + F_{\text{ve}}(\delta,\gamma) + F_{\text{em}}(\delta, V_1, V_2) = F_{\text{int}} \tag{21}$$

As an example, Figs. 5(a) and 5(b) report the simulated Force-Position (FP) curves of the prototype actuator for two

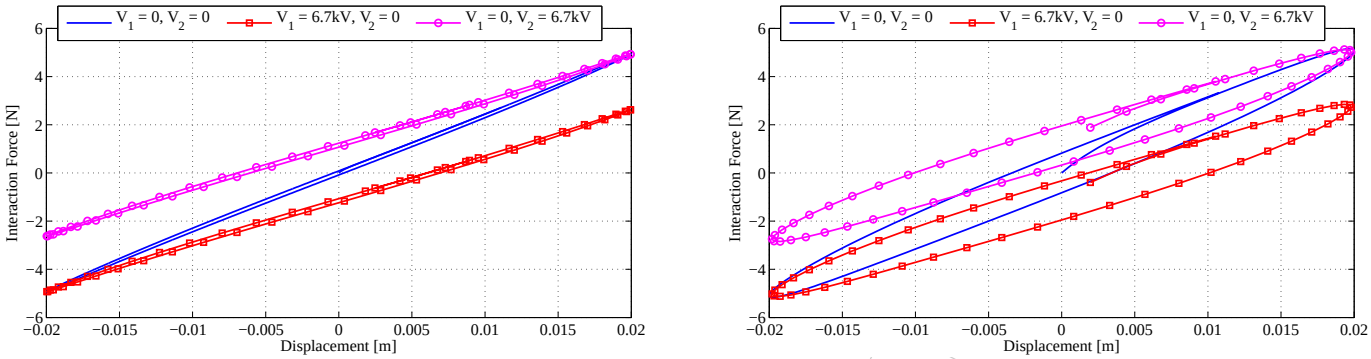

Figure 5. Actuator response for 1mHz (a) and 0.5Hz (b) position cycles

sinusoidal trajectories with $40mm$ amplitude and frequencies equalling $1mHz$ and $0.5Hz$ respectively. The FP curves are computed for the voltage sets $\{V_1 = 0, V_2 = 0\}$ (solid line), $\{V_1 = 6.7kV, V_2 = 0\}$ (circle marks) and $\{V_1 = 0, V_2 = 6.7kV\}$ (dotted line), in case of negligible inertial load and negligible interaction force ($m \approx 0$ and $F_{int} \approx 0$). These plots highlight that, within the considered range of motion, the quasi-static response of the considered DE actuator is rather elastic and linear, whereas its dynamic behavior is severely affected by the hysteresis of the acrylic elastomeric material, which worsens the actuator response as the motion speed increases. This time-dependent effect renders actuator control very challenging and, in practice, limits the functioning of this prototype to applications involving movements with limited dynamics (less than 0.5Hz position cycles). For larger movement dynamics, different DE materials, such as silicone elastomers, should be employed.

4 CONTROL SYSTEM

Recalling Eq. 20, for control purposes, it is now convenient to make a change of variables for the system inputs by posing $u_1 = V_1^2$ and $u_2 = V_2^2$. This assumption implies that the inputs must be non-negative, fact that will define the operative limits of the system as detailed in the following.
The state vector of the system can be then expressed as $z = [\delta\ \dot{\delta}\ \gamma]^T$, the input vector is $u = [u_1\ u_2\ F_{\text{int}}]^T$ where F_{int} is considered as a non-controllable but measurable input, and the output is $y = [\delta]$. The whole system dynamics can be then written as:

$$\dot{z} = f(z) + g(z)u \tag{22}$$
$$y = h(z) + l(z)u \tag{23}$$

An important point to note is that the system is fully observable form the output δ. This can be verified by denoting as $\Delta = [\delta\ \dot{\delta}\ \cdots\ \delta^{(2+r-1)}]^T$ the vector of the time derivative of the DE displacement, and computing the derivative of Δ with respect to the system state

$$\frac{d\Delta}{dz} = \begin{bmatrix} 1 & 0 & 0 \\ 0 & 1 & 0 \\ 0 & 0 & C_{\text{ve}} \\ \star & \star & C_{\text{ve}}\,A_{\text{ve}} \\ & \cdots & \\ \star & \star & C_{\text{ve}}\,A_{\text{ve}}^{r-1} \end{bmatrix} \tag{24}$$

that gives the observability matrix of the system (the stars denote non-meaningful values). Since this matrix is full rank, the system is fully observable. It is then possible to assume the complete knowledge of the system state as the result of the state estimation by means of a properly designed observer. Given this property, it is possible to define as control objective the regulation of the actuator impedance, and in particular of the interaction force F_{int} and of the position δ (or, in other words, the stiffness S) of the DE actuator compensating for the viscous DE actuator behavior. Then, the control objective can be achieved by posing:

$$F_{\text{em}}(\delta, V_1, V_2) = -F_{\text{ve}}(\delta, \gamma) - m\ddot{\delta}_d + b(\dot{\delta} - \dot{\delta}_d) + S_d(\delta - \delta_d) \tag{25}$$

It is important to note that, whence the viscoelastic effect of the DE films has been compensated, from Eq. 20 and 25 the stiffness of the DE actuator results $\alpha[u_1 + u_2] = S_d$. Then, putting Eq. 20 and 25 together:

$$\alpha d[-u_1 + u_2] + \alpha\delta[u_1 + u_2] = -F_{\text{ve}}(\delta, \gamma) + b(\dot{\delta} - \dot{\delta}_d) - m\ddot{\delta}_d + S_d(\delta - \delta_d) \tag{26}$$
$$\alpha[u_1 + u_2] = S_d \tag{27}$$

where $\delta_d, \dot{\delta}_d, \ddot{\delta}_d$ define the desired displacement trajectory. By denoting the displacement error as $e = \delta - \delta_d$, the DE actuator

dynamics becomes:

$$m\ddot{e} + b\dot{e} + S_d e = F_{\text{int}} \tag{28}$$

It follows that the value of the inputs u_1 and u_2 is

$$u_1 = \frac{F_{\text{ve}}(\delta,\gamma) + b(\dot{\delta} - \dot{\delta}_d) + m\ddot{\delta}_d + S_d(d + 2\delta - \delta_d)}{2\alpha d} \tag{29}$$

$$u_2 = \frac{-F_{\text{ve}}(\delta,\gamma) - b(\dot{\delta} - \dot{\delta}_d) - m\ddot{\delta}_d + S_d(d - 2\delta + \delta_d)}{2\alpha d} \tag{30}$$

Now, considering that $V_1 = \sqrt{u_1}$, $V_2 = \sqrt{u_2}$, the control is admissible iff $u_1, u_2 > 0$, that means the desired stiffness should be large enough and the desired displacement small enough for the control system to operate properly. A possible way automatically satisfy this condition is to inscrease the desired stiffness in case one (or both) of the two inputs u_1 or u_2 become lower than zero:

$$\sigma = \max_{i=1,2} u_{\min} - u_i \tag{31}$$

$$u_i = \begin{cases} u_i & \text{if } \sigma < 0 \\ u_i + \sigma & \text{if } \sigma > 0 \end{cases} \qquad i = 1,2 \tag{32}$$

where $\sqrt{u_{\min}} \geq 0$ is the desired minimum value of the input voltage.

The designed controller has then been tested in different conditions by means of simulations. In Fig. 6, the response of the system in case of a large value of the damping coefficient $b = 50$Ns/m and null interaction force is reported. In this simulation the desired stiffness is selected to be a sinusoid with mean value 25N/m and amplitude 12.5N/m. From these plots it is possible to see that, as long as the stiffness is sufficiently high to guarantee the inputs voltage to be strictly positive, the system follows the desired dynamics, imposed by the parameters S_d and b, whereas if the desired stiffness is too small, the control system reacts by increasing the actuator stiffness. Indeed, in this condition, one of the two inputs reaches the desired minimum value (1V in the reported simulations). It is also worth noticing that, from the last plot, the change in the desired stiffness does not influence the viscoelastic force of the DE acutator. The second simulation reported in Fig. 7 shows the response of the system with the same desired position and stiffness trajectory but with a lower value of the damping coefficient $b = 10$Ns/m. It is possible to note from these plots that the response of the system is faster but also the imposed changes in the desired stiffness are larger to allow maintaining positive values of the input voltages. Finally, in Fig. 8 the response of the DE actuator in case of non-null interaction force with constant desired stiffness $S_d = 50$N/m and damping $b = 10$Ns/m is reported. In this case, from the position

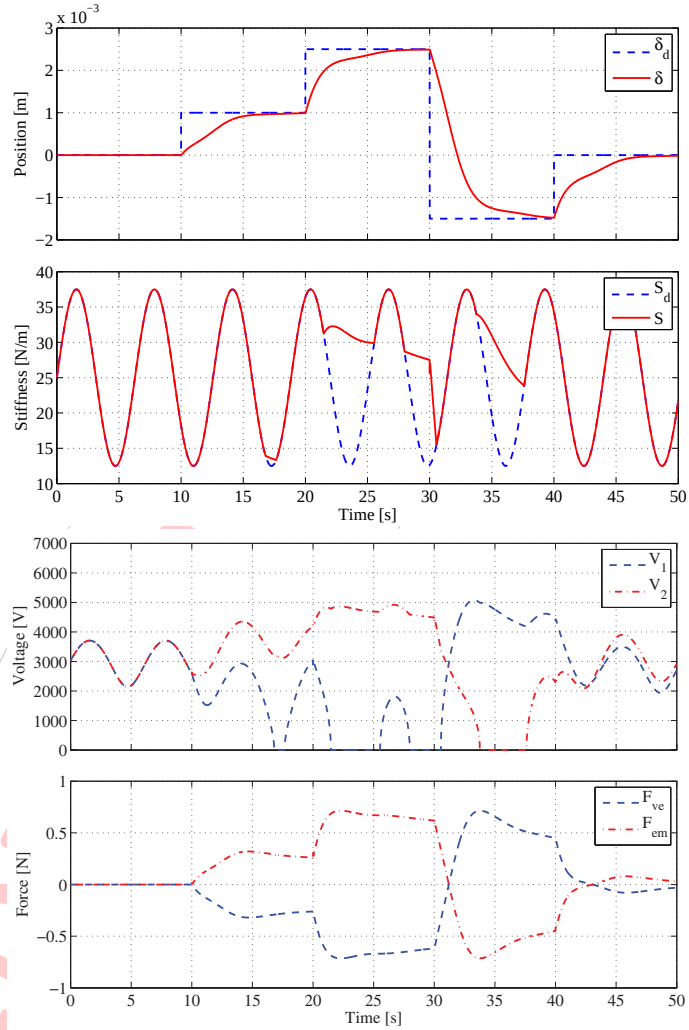

Figure 6. Response of the DE actuator with large value of the damping coefficient b.

error plot, it is important to see that the steady state displacement caused by the interaction force is exactly the value that it can be expected given the desired stiffness of the actuator, while the transient response is governed by the damping coefficient. Moreover, in case of a large and abrupt change in the desired position, as for $t = 30$s, the control system automatically increase the actuator stiffness to ensure positive input voltages.

4.1 Compensation of Model Uncertainties

In case of model uncertainties, in particular for what is related to the viscoelastic model of the DE films, the ideal behavior of the system can be recovered, at least within a certain frequency range, by means of a proper disturbance estimation algorithm based on the system generalized momenta [32, 33]. This estimation algorithm relies on the desired DE actuator dynamics

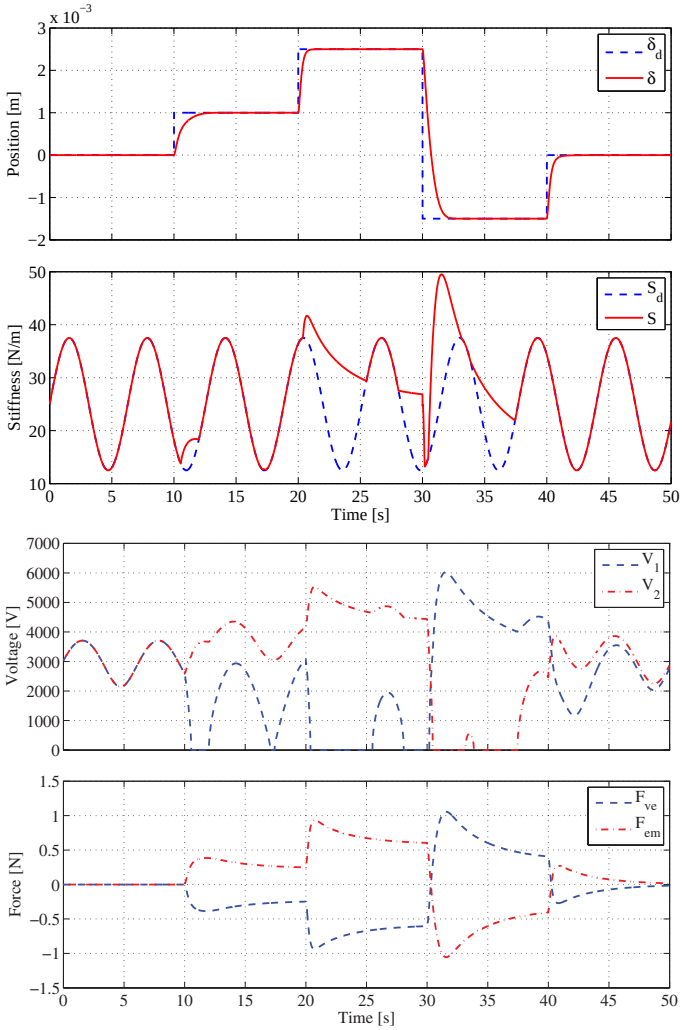

Figure 7. Response of the DE actuator with small value of the damping coefficient b.

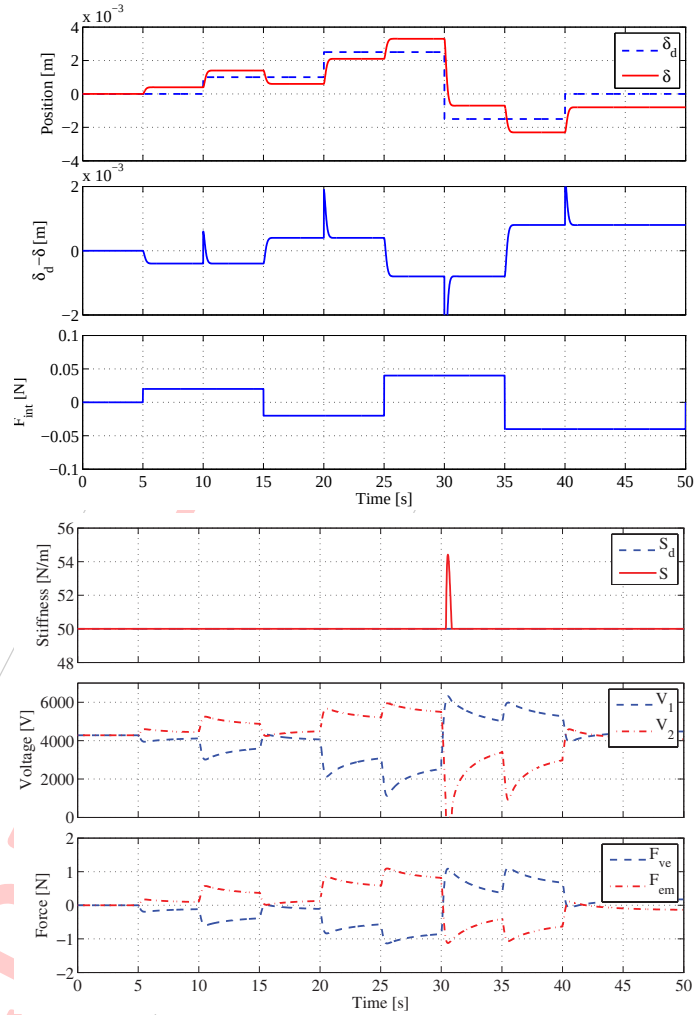

Figure 8. Response of the DE actuator in case of non-null interaction force.

(28). The generalized momenta of the DE actuator can be then expressed as:

$$p = m\dot{\delta} \tag{33}$$

Note that p can be measured knowing the actuator velocity together with its own inertia. In particular, the actuator velocity can be recostructed by digital filtering from the position information, or can be estimated by means of the same observer used for the estimation of the DE internal state γ. Then assuming that no other external force is acting on the system the interaction force apart (since F_{int} is measureable), the DE actuator dynamics can be written as the time derivative of the generalized momenta

$$\dot{p} = m\ddot{\delta} = m\ddot{\delta}_d - b\dot{e} - S_d e + F_{\text{int}} + F_{\text{dist}} \tag{34}$$

where F_{dist} represents the effect of the model uncertainties. Then, by assuming the disturbance estimation law

$$\hat{F}_{\text{dist}} = -L\left[\int\left(m\ddot{\delta}_d - b\dot{e} - S_d e + F_{\text{int}} + \hat{F}_{\text{dist}}\right)dt - p\right] \tag{35}$$

the disturbance estimation dynamics becomes

$$\dot{\hat{F}}_{\text{dist}} = L\left(F_{\text{dist}} - \hat{F}_{\text{dist}}\right) \tag{36}$$

For a better understanding of the estimation algorithm, it is possible to write the transfer function between the disturbance force and its estimated value as

$$\hat{F}_{\text{dist}}(s) = \frac{L}{s+L}F_{\text{dist}}(s) \tag{37}$$

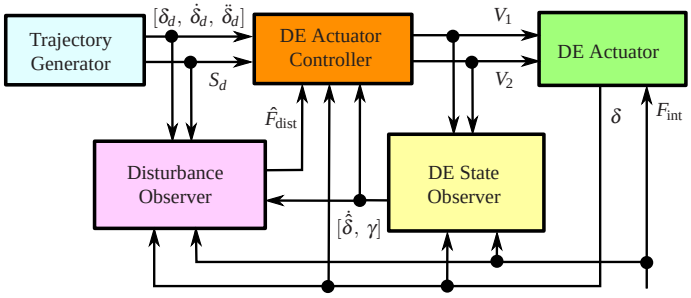

Figure 9. Scheme of the overall DE actuator controller.

From this transfer function it is possible to note that $\hat{F}_{\text{dist}}$ represents a filtered version (through a first order filter which bandwidth determined by $L > 0$) of the disturbance force acting on the DE actuator. The disturbance estimation algorithm can be then rewritten as:

$$\dot{\hat{p}} = m\ddot{\delta}_d - b\dot{e} - S_d e + F_{\text{int}} + \hat{F}_{\text{dist}} \tag{38}$$

$$\hat{F}_{\text{dist}} = -L(\hat{p} - p) \tag{39}$$

The compensation of the disturbance force can be then achieved, within the bandwidth of the trasfer function (37), by including the estimated disturbance into the desired DE actuation force (25). A schematic representation of the overall DE actuator controller is depicted in Fig. 9, whereas Fig. 10 shows the DE actuator response in case of non-null interaction force, constant desired stiffness $S_d = 50$N/m and damping $b = 10$Ns/m, model uncertainties and a value of $L = 100\ \text{s}^{-1}$. These plots show that, in almost all the working conditions (the fast disturbance force transient apart), the DE actuator behaves as in the ideal case where model uncertainties are neglected. In particular, the last plot shows the effective disturbance force F_{dist} the estimated one $\hat{F}_{\text{dist}}$ and the estimation error $F_{\text{dist}} - \hat{F}_{\text{dist}}$, highlighting the effectiveness of the proposed algorithm in estimating the effects of the model uncertainties.

5 CONCLUSIONS

In this paper, the design of an impedance controller for a linear actuator based on a couple of conically-shaped Dielectric Elastomer films in agonist-antagonist configuration has been addressed. The visco-hyperelastic behavior of the polymeric material and the force generated by the electric field on the DE films have been accurately modeled, and an observer able to estimated the DE actuator state has been defined. The designed controller then shapes the DE actuator impedance by: 1) implementing a reciprocal activation strategy of the agonist-antagonist DE films; 2) compensating for the DE intrinsic viscoelasticity; 3) modulating the actuator stiffness according to the operative limits of the

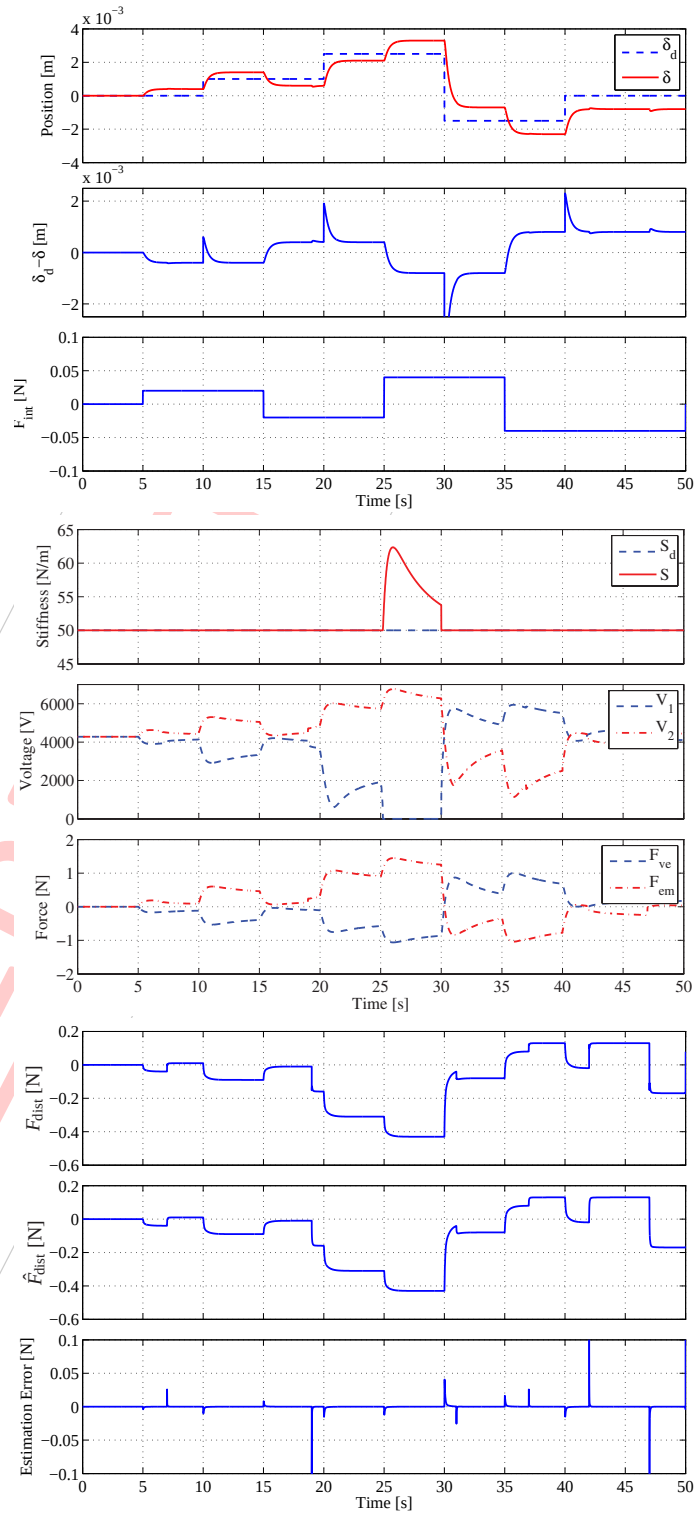

Figure 10. Response of the DE actuator in case of model uncertainties.

systems (e.g. in case the desired stiffness is too small). Finally, a second observer for estimating the effects of model uncertainties has been designed and tested. The developed control system requires the measurement of the DE actuator displacement and interaction force. Future activities will be devoted to the experimental validation of the proposed controller.

REFERENCES

[1] Yuta, S., Asama, H., Thrun, S., Prassler, E., and Tsubouchi, T., 2006. *Field and Service Robotics - Recent Advances in Research and Applications*. Springer Tracts in Advanced Robotics (STAR).

[2] Haddadin, S., Albu-Schaffer, A., and Hirzinger, G., 2007. "Safety evaluation of physical human-robot interaction via crash-testing". In Proceedings of Robotics: Science and Systems.

[3] Bicchi, A., et al., 2008. "Physical human-robot interaction: Dependability, safety, and performance". In Proc. of the 10th IEEE Int. Workshop on Advanced Motion Control, pp. 9–16.

[4] Gomis-Bellmunt, O., and Campanile, L., 2010. *Design Rules for Actuators in Active Mechanical Systems*. Springer, Berlin.

[5] Russell, D. L., McTavish, M., and English, C. E., 2009. "Mechanical issues inherent in antagonistically actuated systems". *ASME Transactions, Journal of Mechanisms and Robotics*, ***1***(4), p. 044501(8).

[6] Hogan, N., 1984. "Adaptive control of mechanical impedance by coactiva- tion of antagonist muscles". *IEEE Transacation on Automatic Control*, ***29***(8), pp. 681–690.

[7] Shen, X., and Goldfarb, M., 2007. "Simultaneous force and stiffness control of a pneumatic actuator". *Journal of Dynamic Systems, Measurement, and Control*, ***129***, pp. 425–434.

[8] Nigg, B., and Liu, W., 1999. "The effect of muscle stiffness and damping on simulated impact force peaks during running". *Journal of Biomechanics*, ***32***(8), pp. 849–856.

[9] Dastoor, S., and Cutkosky, M., 2011. "Variable impedance due to electromechanical coupling in electroactive polymer actuators". In Intelligent Robots and Systems (IROS), 2011 IEEE/RSJ International Conference on, pp. 774–779.

[10] Alexander, R., 1990. "Three uses for springs in legged locomotion". *International Journal of Robotic Research*, ***9***(2), pp. 53–61.

[11] Bicchi, A., and Tonietti, G., 2004. "Fast and soft arm tactics: Dealing with the safety-performance trade-off in robot arms design and control". *IEEE Robotics and Automation Magazine*, ***11***(2), pp. 22–33.

[12] Palli, G., and Melchiorri, C., 2011. "Output-based control of robots with variable stiffness actuation". *Journal of Robotics*, ***2011***, pp. 1–15.

[13] Sardellitti, I., Palli, G., Tsagarakis, N., and Caldwell, D., 2010. "Antagonistically actuated compliant joint: Torque and stiffness control". In IEEE/RSJ IROS Int. Conf. on Intelligent Robots and Systems, pp. 1909 –1914.

[14] Migliore, S. A., Brown, E. A., and DeWeerth, S. P., 2007. "Novel nonlinear elastic actuators for passively controlling robotic joint compliance". *Journal of Mechanical Design*, ***129***(4), pp. 406–412.

[15] Schiavi, R., Grioli, G., Sen, S., and Bicchi, A., 2008. "VSA-II: a novel prototype of variable stiffness actuator for safe and performing robots interacting with humans". In IEEE ICRA Int. Conf. on Robotics and Automation.

[16] Palli, G., Berselli, G., Melchiorri, C., and Vassura, G., 2011. "Design of a variable stiffness actuator based on flexures". *ASME Transactions, Journal of Mechanisms and Robotics*, ***3***(3), p. 034501(5).

[17] Ham, R., Sugar, T., Vanderborght, B., Hollander, K., and Lefeber, D., 2009. "Compliant actuator designs". *IEEE Robotics Automation Magazine*, ***16***(3), pp. 81 –94.

[18] Quy, H. V., Aryananda, L., Sheikh, F., Casanova, F., and Pfeifer, R., 2011. "A novel mechanism for varying stiffness via changing transmission angle". In IEEE ICRA Int. Conf. on Robotics and Automation, pp. 5076 –5081.

[19] Fauteux, P., Lauria, M., Heintz, B., and Michaud, F., 2010. "Dual-differential rheological actuator for high-performance physical robotic interaction". *Robotics, IEEE Transactions on*, ***26***(4), pp. 607–618.

[20] Son, S., and Goulbourne, N., 2009. "Finite deformations of tubular dielectric elastomer sensors". *Journal of Intelligent Material Systems and Structures*, ***20***(18), pp. 2187–2199.

[21] Vertechy, R., Fontana, M., Rosati-Papini, G., and Bergamasco, M., 2013. "Oscillating-water-column wave-energy-converter based on dielectric elastomer generator". In Proc. SPIE 8687, Electroactive Polymer Actuators and Devices (EAPAD), p. 86870I.

[22] Vertechy, R., Bergamasco, M., Berselli, G., Castelli, V. P., and Vassura, G., 2012.. "Compliant actuation based on dielectric elastomers for a force-feedback device: Modeling and experimental evaluation". *Frattura ed Integrita Strutturale*, ***23***, pp. 47–56.

[23] He, T., Zhao, X., and Suo, Z., 2009. "Equilibrium and stability of dielectric elastomer membranes undergoing inhomogeneous deformation". *Journal of Applied Physics*, ***106***, p. 083522.

[24] Vertechy, R., Frisoli, A., Bergamasco, M., Carpi, F., Frediani, G., and Rossi, D. D., 2012. "Modeling and experimental validation of buckling dielectric elastomer actuators". *Smart Materials and Structures*, ***21***(9), p. 094005.

[25] Berselli, G., Vertechy, R., Vassura, G., and Castelli, V. P., 2011. "Optimal synthesis of conically-shaped dielectric elastomer linear actuators: Design methodology and experimental validation". *IEEE/ASME Transactions*

on Mechatronics, DOI: 10.1109/TMECH.2010.2090664, ***16***(1), pp. 67 –79.

[26] Kofod, G., 2008. "The static actuation of dielectric elastomer actuators: how does pre-stretch improve actuation?". *J. Phys. D: Appl. Phys.*, ***41***, p. 215405 (11pp).

[27] Vertechy, R., Berselli, G., Parenti Castelli, V., and Bergamasco, M., 2013. "Continuum thermo-electro-mechanical model for electrostrictive elastomers". *Journal of Intelligent Material Systems and Structures*, ***24***(6), pp. 761–778.

[28] Berselli, G., Vertechy, R., Vassura, G., and Parenti Castelli, V., 2011. "Optimal synthesis of conically-shaped dielectric elastomer linear actuators: Design methodology and experimental validation". *IEEE/ASME Transactions on Mechatronics*, ***16***(1), pp. 67 –79.

[29] Fung, Y. C., 1993. *Biomechanics: Mechanical Properties of Living Tissues*. Springer-Verlag, Berlin.

[30] Findley, W. N., Lai, J. S., and Onaran, K., 1989. *Creep and relaxation of nonlinear viscoelastic materials: with an introduction to linear Viscoelasticity*. Dover pubblications, New York.

[31] Yeoh, O. H., 1990. "Characterization of elastic properties of carbon-black-filled rubber vulcanizates". *Rubber Chemistry and Technology*, ***63***, pp. 792–805.

[32] De Luca, A., and Mattone, R., 2003. "Actuator failure detection and isolation using generalized momenta". In Proc. IEEE Int. Conf. on Robotics and Automation.

[33] Palli, G., and Melchiorri, C., 2008. "Velocity and disturbance observer for non-model based load and friction compensation". In Proc. Int. Workshop on Advanced Motion Control, pp. 194–199.